Proceedings of the 27th International Symposium on Power Semiconductor Devices & IC's
May 10-14, 2015, Kowloon Shangri-La, Hong Kong

Predictive and Efficient Modeling of Hot-Carrier Degradation in nLDMOS Devices

Prateek Sharma•, Stanislav Tyaginov*,†, Yannick Wimmer•, Florian Rudolf*, Karl Rupp*, Markus Bina*,
Hubert Enichlmair°, Jong-Mun Park°, Hajdin Ceric•, and Tibor Grasser*
•Christian Doppler Laboratory at the *Institute for Microelectronics, Technische Universität Wien, 1040 Vienna, Austria
†Ioffe Physical-Technical Institute, 194021 St. Petersburg, Russia
°ams AG, Unterpremstätten, Austria
Email:sharma@iue.tuwien.ac.at

***Abstract*—We present a physical model for hot-carrier degradation (HCD) which is based on the information provided by the carrier energy distribution function. In the first version of our model the distribution function is obtained as the exact solution of the Boltzmann transport equation, while in the second one we employ the simplified drift-diffusion scheme. Both versions of the model are validated against experimental HCD data in nLDMOS transistors, namely against the change of such device characteristics as the linear and saturation drain currents. We also compare the intermediate results of these two versions, i.e. the distribution function, defect generation rates, and interface state density profiles. Finally, we make a conclusion on the vitality of the drift-diffusion based version of the model.**

***Index Terms*—hot-carrier degradation, nLDMOS, spherical harmonics expansion, drift-diffusion scheme**

I. Introduction

Although hot-carrier degradation (HCD) is known to be one of the most important reliability concerns in modern microelectronic devices [1], the full physical picture behind this detrimental phenomenon is very complicated. As a result, predictive modeling of HCD is difficult and very often simplified empirical/phenomenological approaches are used [2]. This is because – depending on the applied stress voltages – HCD can be driven by "hot" or "colder" carriers, which trigger the single- and multiple-carrier mechanisms of Si-H bond dissociation [3]–[6]. The rates of these competing processes are determined by the carrier energy distribution function (DF). To obtain this DF one needs to solve the Boltzmann transport equation, which is computationally quite demanding [7]. As a result, the most dramatic simplification which is often made in HCD models is to avoid the thorough evaluation of the carrier energy distribution function and to use, instead, some empirical parameters based on the macroscopic device characteristics [8]–[11]. However, as we have recently demonstrated, a comprehensive HCD model needs to be based on a proper carrier transport treatment [5]. Therefore, these simplified approaches are not predictive when the transition from accelerated hot-carrier stress to real operating condition results in a change of the dominant physical mechanism of HCD.

The situation becomes even more dramatic in the case of an LDMOS transistor, which has a sophisticated architecture (including the bird's beak and curved interface, see Fig. 1) and high operating voltages, which makes a proper treatment of carrier transport challenging. Furthermore, as recently shown by our group [12], both the single- and multiple-carrier bond-breakage process have to be considered even for such a large device to properly capture the degradation, thus making the predictive modeling a challenging task. At the same time, the LDMOS device is very attractive for mixed-signal integrated circuits and high-voltage automotive applications [13], and thus predictive modeling of HCD in these transistors is of great importance. We present an HCD model based on a thorough solution of the Boltzmann transport equation by means of the spherical harmonics expansion (SHE) approach as well as a simplified version which relies on "classical" drift-diffusion (DD) simulations and check the limits of this approach.

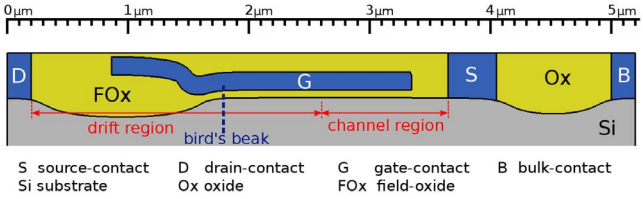

Fig. 1: The schematic representation of the near-interface section of the nLDMOS with all the characteristic sections labeled.

II. Experiment

Experiments are performed using nLDMOS transistors fabricated in a 0.35 μm process (the device is sketched in Fig. 1) which were subjected to hot-carrier stress with six different combinations of drain and gate voltages $V_{\rm ds}$, $V_{\rm gs}$ (i.e. at $V_{\rm gs}$ = 2.0 V and $V_{\rm ds}$ = 18, 20, 22 V; $V_{\rm ds}$ = 20 V; $V_{\rm gs}$ = 1.2, 1.5, 2.0 V) at room temperature for $\sim$1 Ms. The Si/SiO_2 interface length is $\sim$3.4 μm, while the gate length is $\sim$2.5 μm. To assess HCD, the change in the linear drain current $\Delta I_{\rm d,lin}$ (at $V_{\rm ds}$ = 0.1 V and $V_{\rm gs}$ = 2.4 V) and saturation drain current $\Delta I_{\rm d,sat}$ (at $V_{\rm ds}$ = 10 V and $V_{\rm gs}$ = 3.6 V) was recorded as a function of stress time ($\Delta I_{\rm d,lin}(t)$ and $\Delta I_{\rm d,sat}(t)$). Note that we consider the normalized (to the value typical for the pristine transistor) change of these quantities.

III. Model Details

Our HCD model consolidates three main sub-modules: carrier transport treatment, a description of the microscopic mechanism of defect generation, and modeling of the degraded

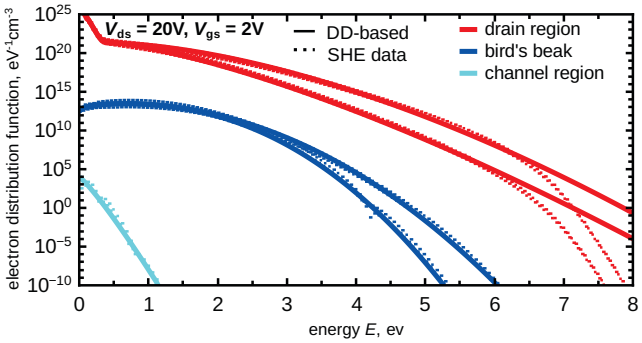

Fig. 2: Comparison of DFs from the DD-based model with those obtained from ViennaSHE for stress voltages: $V_{\rm ds}$ = 20 V, $V_{\rm gs}$ = 2 V, calculated near the drain, bird's beak and channel regions.

devices [5], [6]. The model is implemented in the deterministic Boltzmann transport equation solver ViennaSHE [14]. ViennaSHE evaluates the carrier DFs for the given device structure and defined stress/operating conditions, see Fig. 2. The transistor architecture is obtained using the Sentaurus Process simulator [15]. Since the carrier DFs are sensitive to the device doping profiles, the process and device simulators are calibrated in a coupled manner to reproduce the characteristics of the fresh nLDMOS. It is important to emphasize that even a simplified DD approach to the Boltzmann transport equation solution can be computationally challenging in such a device as the nLDMOS. For instance, this transistor has high doping gradients in the vicinity of the Si/SiO_2 interface, while near the bulk electrode, the doping is almost constant. As a result, a highly adaptive meshing is needed. For this purpose, we used the ViennaMesh [16] framework which generates meshes using the built-in potential, see Fig. 3. The mesh thus generated has a fine resolution in important regions, and sufficiently low density in less important areas so that all the vital characteristics of the device are captured at reduced computational cost. The HCD model incorporates such important ingredients as the self-consistent consideration of single- and multiple-carrier mechanisms of Si-H bond-breakage, the reduction of the bond rupture activation energy due to the interaction of the dipole moment of the bond with the electric field, and statistical fluctuations of this energy. The rates of both the single- and multiple-carrier process are determined by the carrier acceleration integral [5], [6]:

$$I^{\rm e/h}_{\rm SC/MC} = \int_0^\infty f(\varepsilon) g(\varepsilon) v(\varepsilon) \sigma_0 (\varepsilon - \varepsilon_{th})^p d\varepsilon, \qquad (1)$$

where f is the carrier energy DF, g the density-of-states, $v(\varepsilon)$ the carrier group velocity, and $\sigma_0(\varepsilon - \varepsilon_{th})^p$ the reaction cross section. The product $f(E)g(E)v(E)$ represents the number of carriers impinging on the interface per unit time and per unit area, while the reaction cross section determines the probability that this particular particle from the ensemble was successful to dissociate the bond.

The idea to avoid the computationally expensive SHE simulations and employ instead the simplified DD scheme appears to be very attractive, especially in the case of an nLDMOS transistor [17]. We estimate the DFs from the DD solution using the analytical expression (2) [18]

$$f(\varepsilon) = A \exp\left[-\left(\frac{\varepsilon}{\varepsilon_{\rm ref}}\right)^b\right] + C \exp\left[-\frac{\varepsilon}{k_{\rm B} T_n}\right], \qquad (2)$$

where $k_{\rm B}$ is the Boltzmann constant, and T_n the carrier temperature. The parameters of the DF are determined using information on the moments of the Boltzmann transport equation, i.e the local carrier concentration and carrier temperature, see (3). The electric field profile $F(x)$ from DD-simulations, for the given stress voltages, is used to find the carrier temperature, $T(x)$, according to:

$$T_{\rm n} = T_{\rm L} + \frac{2}{3}\frac{q}{k_{\rm B}} \tau \mu F^2, \qquad (3)$$

where $T_{\rm L}$ is the lattice temperature, q the modulus of the electron charge, and τ the energy relaxation time. The parameters of the DF are then obtained from the solution of the following set of integral equations:

$$\int_0^\infty f(\varepsilon) g(\varepsilon) d\varepsilon = n \qquad (4)$$

$$\int_0^\infty \varepsilon f(\varepsilon) g(\varepsilon) d\varepsilon = \frac{3}{2} n k_{\rm B} T_{\rm n} \qquad (5)$$

$$\int_0^\infty f(\varepsilon) d\varepsilon = 1. \qquad (6)$$

To describe the bond dissociation kinetics we use a truncated harmonic oscillator model of the Si-H bond [3]–[6]. We consider all possible superposition of the single- and multiple-carrier processes of the bond dissociation. The rates of the multiple-carrier process are modeled as

$$P_{\rm u} = I_{\rm MC} + \omega_{\rm e} \exp[-\hbar\omega / k_{\rm B} T_{\rm L}], \qquad (7)$$

$$P_{\rm d} = I_{\rm MC} + \omega_{\rm e}, \qquad (8)$$

where $P_{\rm u}$, $P_{\rm d}$ are bond excitation/deexcitation rates, $\omega_{\rm e}$ is the oscillator vibrational frequency, while $\hbar w$ is the distance between the oscillator levels.

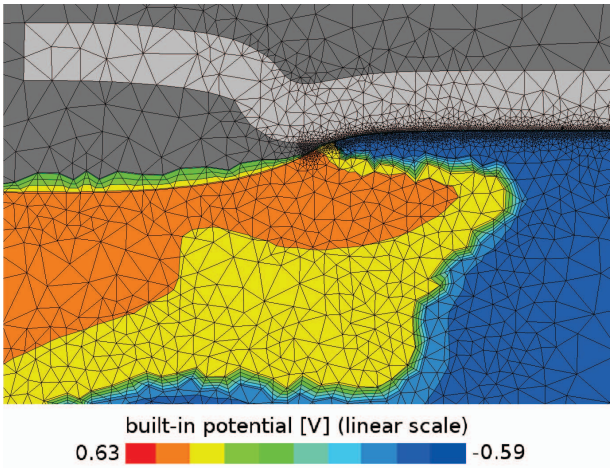

Fig. 3: The adaptive meshing tool, ViennaMesh, modulates the mesh density based on the built-in potential. The mesh is fine near the Si/SiO_2 interface and coarse in the Si bulk.

We assume that the bond-dissociation event can occur from any oscillator level with the corresponding rate:

$$R_{\mathrm{a},i} = \omega_{\mathrm{th}} \exp[-(E_a - E_i)/k_{\mathrm{B}}T_{\mathrm{L}}] + AI_{\mathrm{SC},i}, \qquad (9)$$

where the first term corresponds to the thermal activation of the hydrogen atom over the potential barrier between the bonded state and the transport mode, while the second term represents the effect of hot carriers. The cumulative bond-breakage rate is calculated as a sum of the rates from all particle levels weighted with the corresponding occupation numbers:

$$\Re_{\mathrm{a}} = \frac{1}{k}\sum_{r=0} R_{\mathrm{a},i}\left(\frac{P_{\mathrm{u}}}{P_{\mathrm{d}}}\right). \qquad (10)$$

As for the rate of the bond passivation reaction $\Re_{\mathrm{p}}$, for the sake of simplicity, we model this process as a thermal activation over the barrier E_{p} with the corresponding attempt frequency ν_{p}:

$$\Re_{\mathrm{p}} = \nu_{\mathrm{p}} \exp(-E_{\mathrm{p}}/k_{\mathrm{B}}T_{\mathrm{L}}). \qquad (11)$$

The solution of the equation set describing the bond passivation/depassivation processes leads to an analytic expression for the interface state density (12):

$$\begin{aligned} N_{\mathrm{it}} &= \frac{\sqrt{\Re_{\mathrm{a}}^2/4 + N_0\Re_{\mathrm{a}}\Re_{\mathrm{p}}}}{\Re_{\mathrm{p}}}\frac{1-f(t)}{1+f(t)} - \frac{\Re_{\mathrm{a}}}{2\Re_{\mathrm{p}}}, \\ f(t) &= \frac{\sqrt{\Re_{\mathrm{a}}^2/4 + N_0\Re_{\mathrm{a}}\Re_{\mathrm{p}}} - \Re_{\mathrm{a}}/2}{\sqrt{\Re_{\mathrm{a}}^2/4 + N_0\Re_{\mathrm{a}}\Re_{\mathrm{p}}} + \Re_{\mathrm{a}}/2} \times \\ &\quad \times \exp\left(-2t\sqrt{\Re_{\mathrm{a}}^2/4 + N_0\Re_{\mathrm{a}}\Re_{\mathrm{p}}}\right). \end{aligned} \qquad (12)$$

The interface state density profiles $N_{\mathrm{it}}(x)$ computed for each stress time step are then loaded to the device simulator MiniMOS-NT [19] to simulate the degradation traces of the device characteristics ($\Delta I_{\mathrm{d,lin}}$ and $\Delta I_{\mathrm{d,sat}}$).

IV. Results and Discussion

Fig. 2 presents a family of DFs simulated for V_{ds} = 20 V and V_{gs} = 2.0 V using the SHE- and DD-based versions of the model. The DFs are plotted near the drain, near the bird's beak, and in the channel. The two former ones are severely non-equilibrium, while the latter one is almost Maxwellian. The DFs obtained using the DD-based approach agree well with those obtained with ViennaSHE. A small discrepancy is visible at high energies in the drain region. At these high energies, however, DF values drop by more than 20 orders of magnitude and this discrepancy does not transform into a significant error in the model. To prove this we also plot the acceleration integral for the single-carrier process (Fig. 4) and $N_{\mathrm{it}}(x)$ profiles (Fig. 5). Figs. 4,5 show that the acceleration integrals and the $N_{\mathrm{it}}(x)$ profiles evaluated using the SHE- and DD-based approaches are very similar. The hot carriers near the drain, see Fig. 2, lead to saturation of both the single- and multiple-carrier processes, thus producing the N_{it} peak at the drain region. The peak in the bird's beak region is due to the single-carrier process alone, while the third N_{it} maximum in the channel at $x \sim$2.8 μm is a result of the common action of the multiple-carrier process of the bond dissociation and the

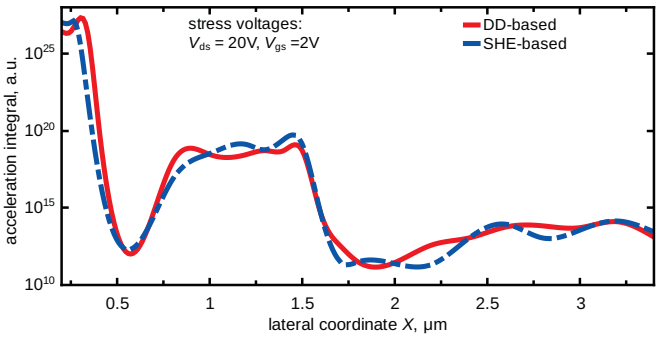

Fig. 4: The acceleration integrals calculated from the DFs obtained from the DD-based model and ViennaSHE for V_{ds} = 20 V, V_{gs} = 2 V.

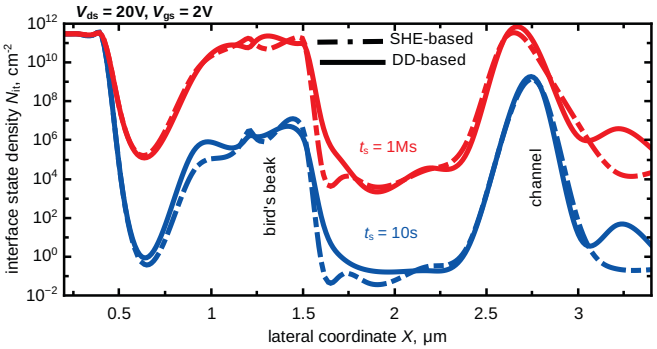

Fig. 5: The interface state densities obtained from the DD-based model and ViennaSHE for V_{ds} = 20 V, V_{gs} = 2 V at 10 s and 1 Ms.

interaction of the dipole moment of the bond with the electric field [12].

The normalized experimental changes of the linear and saturation drain currents plotted vs. the theoretical ones are shown in Fig. 6 for a fixed V_{gs} = 2.0 V and a series of three V_{ds} equal to 18, 20, and 22 V. One can see that agreement between experiment and the model is very good. It is important to emphasize that the $\Delta I_{\mathrm{d,lin}}(t)$ and $\Delta I_{\mathrm{d,sat}}(t)$ curves obtained with the SHE- and DD-based versions of the model are almost the same within the whole experimental time window and that the DD-version can be used for predictive simulations of HCD. To prove this, we also plot normalized current changes simulated with the DD-model, without any additional tuning with the SHE-based model, for fixed V_{ds} = 20 V and three different V_{gs} = 1.2, 1.5, and 2.0 V, see Fig. 7. Fig. 7 shows quite good agreement between the experimental degradation traces and those obtained with the simplified version of the model. We conclude that the DD-based HCD model can properly represent the degradation of such device characteristics as $\Delta I_{\mathrm{d,lin}}$ and $\Delta I_{\mathrm{d,sat}}$.

V. Conclusions

We have presented and verified our physics-based model for HCD against the degradation data measured in nLDMOS transistors. The model employs carrier transport treatment, and has two versions, i.e. based on the exact solution and simplified solution of the Boltzmann transport equation. The first variant uses the spherical harmonics expansion technique whereas the second one relies on a simplified drift-diffusion

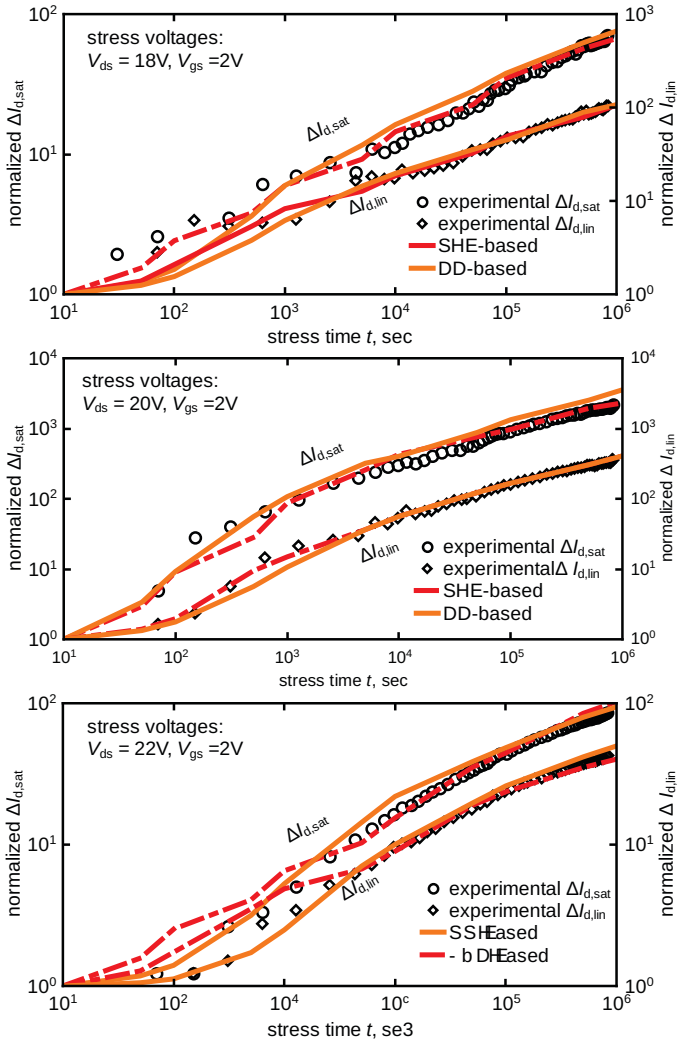

Fig. 6: The experimental change in the saturation and linear drain currents plotted vs. the simulated ones obtained with the SHE- and DD-based models for a fixed gate voltage $V_{\rm gs}$ = 2 V and three different drain voltages $V_{\rm ds}$ = 18, 20 and 22 V.

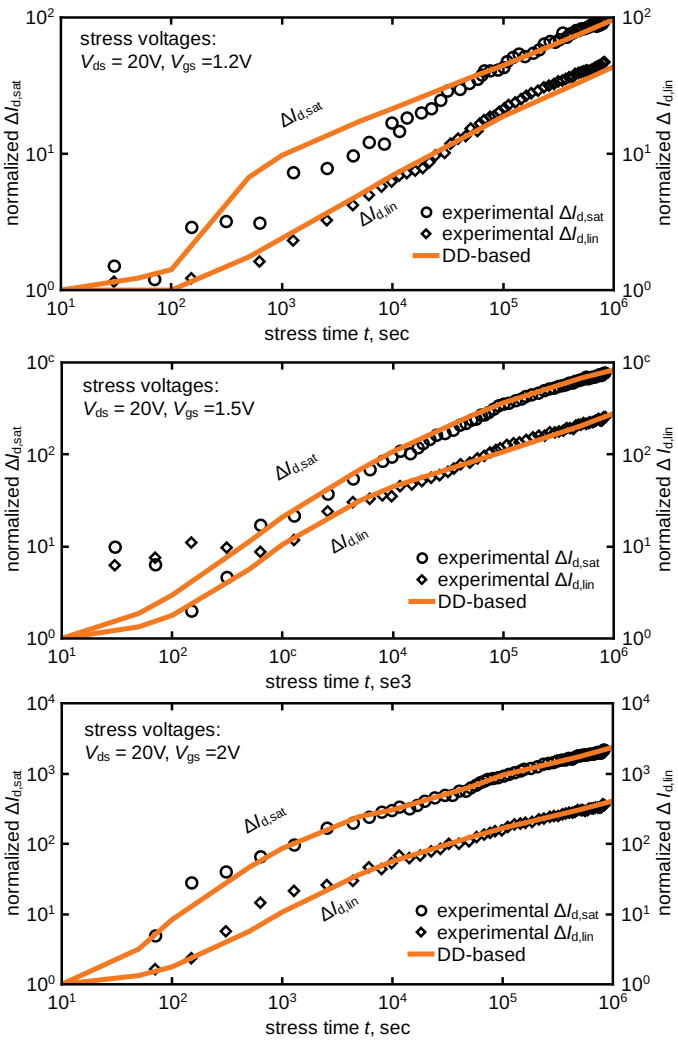

Fig. 7: The change in the saturation and linear drain currents: experiment vs. the DD-based model. Results are obtained for a fixed drain voltage $V_{\rm ds}$ = 20 V and three different gate voltages $V_{\rm gs}$ = 1.2, 1.5 and 2 V.

scheme. These two versions of the model are compared in terms of the carrier distribution functions, defect generation rates, interface state density profiles, and the degradation of such device characteristics as the linear and saturation drain currents. We have demonstrated that all the results of these two versions are very similar. Moreover, both models can successfully represent the experimental degradation traces, i.e. $\Delta I_{\rm d,lin}(t)$ and $\Delta I_{\rm d,sat}(t)$ using the same values of the model parameters. Finally we conclude that the fast and reliable DD-based version of the model is very attractive for predictive HCD simulations in nLDMOS devices.

Acknowledgments

The authors acknowledge support by the Austrian Science Fund (FWF), grant P23598, the European Union FP7 project ATHENIS_3D (grant No 619246), and the European Research Council (ERC) project MOSILSPIN (grant No 247056).

References

[1] *International Technology Roadmap for Semiconductors (ITRS)*, 2013.
[2] S. Tyaginov *et al.*, ECS Transactions **35**, 321 (2011).
[3] W. McMahon *et al.*, *Proc. Int. Conf. Mod. Sim. Micro* (2002), Vol. 1, pp. 576–579.
[4] A. Bravaix *et al.*, *Proc. IRPS* (2009), pp. 531–546.
[5] S. Tyaginov *et al.*, Proc. IRPS, 2014.
[6] M. Bina *et al.*, IEEE Trans. Electron Dev. **61**, 3103 (2014).
[7] C. Jungemann *et al.*, *Hierarchical Device Simulation* (Springer Verlag Wien/New York, 2003).
[8] S. Rauch *et al.*, IEEE Trans. Dev. Material. Reliab. **5**, 701 (2005).
[9] S. Rauch *et al.*, *Proc. IRPS, tutorial* (2010).
[10] C. Guerin *et al.*, IEEE Trans. Dev. Material. Reliab. **7**, 225 (2007).
[11] Y. Randriamihaja *et al.*, Microel. Reliab. **52**, 2513 (2012).
[12] Y. Wimmer *et al.*, Proc. IIRW, in press, 2014.
[13] S. Reggiani *et al.*, Solid-State Electronics, in press, 2014.
[14] *http://viennashe.sourceforge.net/*, 2014.
[15] *Synopsys, Sentaurus Process, Advanced Simulator for Process Technologies*.
[16] *http://viennamesh.sourceforge.net/*, 2014.
[17] S. Reggiani *et al.*, Proc. ISPSD, 2014.
[18] T. Grasser *et al.*, Journ. Appl. Phys. **91**, 3869 (2002).
[19] *MiniMOS-NT Device and Circuit Simulator*, Institute for Microelectronic, TU Wien.